PRAMANA
— journal of
physics

Vol. 78, No. 3
March 2012
pp. 483–492

Magnetic response of split-ring resonator metamaterials: From effective medium dispersion to photonic band gaps

SANGEETA CHAKRABARTI and S ANANTHA RAMAKRISHNA*
Department of Physics, Indian Institute of Technology-Kanpur, Kanpur 208 016, India
*Corresponding author. E-mail: sar@iitk.ac.in

MS received 28 April 2011; accepted 14 October 2011

Abstract. On systematically investigating the electromagnetic response of periodic split-ring resonator (SRR) metamaterials as a function of the size-to-wavelength (a/λ) ratio, we find that the stop bands due to the geometric resonances of the SRR weaken with increasing (a/λ) ratio, and are eventually replaced by stop bands due to Bragg scattering. Our study traces the behaviour of SRR-based metamaterials as the resonance frequency increases and the wavelength of the radiation finally becomes comparable to the size of the unit cell of the metamaterial. In the intermediate stages, the dispersion of the SRR metamaterial can still be described as due to a localized magnetic resonances while Bragg scattering finally becomes the dominant phenomenon as $a/\lambda \sim 1/2$.

Keywords. Metamaterials, split-ring resonators, magnetic resonance.

PACS Nos 78.67.Pt; 42.70.Qs; 41.20.−q

1. Introduction

Materials with a negative index of refraction [1] are an intensely researched topic today. By definition, materials with a negative index of refraction simultaneously possess negative permittivity and negative permeability [2,3]. The metallic split-ring resonator (SRR) was proposed by Pendry *et al* [4] as a means of achieving negative permeability at any desired frequency and has been the basis of most metamaterials ranging from few GHz [5] to near infrared (NIR) [6] frequencies. In this context, it is to be noted that metals possess a negative permittivity at (optical) frequencies, below their plasma frequencies. In addition, dielectric media and structured metamaterials with a dielectric resonance may also possess negative permittivity in a frequency band above a particular resonance frequency [2].

The SRR allows the generation of a magnetic resonance and a negative permeability band which depends on the geometry of the structure. The functioning of SRR-based metamaterials has been explained using an LC-circuit paradigm [4]. SRR, or its variants such as fish-net metamaterials [7], are the primary producers of magnetically active

DOI: 10.1007/s12043-011-0241-x; ***e*Publication: 16 February 2012**

metamaterials. SRR metamaterials were used for the experimental demonstration [8] of electromagnetic invisibility or cloaking [9] too. The idea of the structured composite medium (metamaterial) forming an effective medium which can be described by a negative permeability is one of the most important concepts in this description. Effective medium theories necessarily require that the medium is homogenizable, a condition which can be satisfied for SRRs designed to function at low frequencies when the sizes of the individual unit cells are much smaller compared to the wavelength of the incident radiation. However, as the magnetic resonance frequencies are pushed up higher, the response of the metamaterial starts deviating from the ideal effective medium behaviour. The LC resonance model along with Maxwell's equations implied that the SRR resonance frequency would scale inversely with the size of the SRR. This scaling does not hold at high frequencies when the metallic elements that comprise the SRR structure respond more as plasmas than as Ohmic conductors. It was shown that geometric reduction of the size would eventually lead to a saturation of the SRR resonance frequency [10]. It has been shown that for resonance at near-infrared and optical frequencies, the serial capacitance of the structure would need to be reduced by inserting additional capacitive gaps in the SRR [11]. This, however, leads to an increase in the size vs. wavelength (a/λ) ratio which is undesirable from the perspective of a description by effective medium theories.

In this paper, we investigate how the electromagnetic response of SRR-based metamaterials for negative permeability evolves as changes are made to the structure to decrease the resonance wavelength. The medium progressively becomes less homogenizable and ultimately, the effective medium theories break down. However, even if the size-to-wavelength ratios of these metamaterials make it impossible to homogenize them and describe them by means of effective material parameters, they may still exhibit an overall magnetic response arising due to the plasmonic response of the metallic SRR. At even higher frequencies, the magnetic resonance dies out and Bragg scattering due to the periodic nature of the metamaterial becomes the dominant phenomenon.

2. The magnetic response of SRR-based metamaterials

The equivalent circuit model of the SRR shows that the capacitive gaps in the structure are of the greatest importance in determining its resonance frequency [10]. Indeed, it is much easier to vary the resonance frequency of SRRs by altering the gap width, the number of gaps or the material within the gaps (and hence, the capacitance), than by altering the inductance. The sensitivity of SRRs to varying gap widths and its effect on the effective medium response has been presented in this paper. The electromagnetic responses of a variety of SRR-based metamaterial structures were simulated and the gradual change in their electromagnetic responses, with changes in their geometric structures, were studied. The photonic band structures, along with the reflectivity and the transmittivity, were calculated for slabs of the metamaterial consisting of four layers of unit cells. The responses of these media show a variety of phenomena as one progresses from the effective medium behaviour of the metamaterial, through the weakening and the breakdown of this picture, to the limit of large unit cells where the length scales involved ($a \sim \lambda/2$) lead to the conclusion that Bragg scattering is responsible for the formation of the band gap. The wave

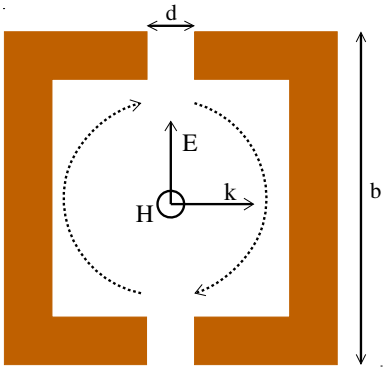

Figure 1. Schematic diagram of the SRR whose electromagnetic response with varying d has been studied in this paper. The side of the unit cell is $a = 300$ nm, while the sides of the SRR are 180 nm long.

impedance (defined as $Z = \sqrt{\mu/\epsilon}$) calculated for each of these structures, gives an idea of the nature of the response of the medium at frequencies near the band gap(s). When the wavelength at resonance is large compared to the unit cell size, the metamaterial can be treated as a homogeneous medium near the band-gap (resonant) frequency. In such cases, effective material parameters can be assigned to it, uniquely characterizing the origin of its response as electric or magnetic in nature. If the medium cannot be homogenized, field maps of the electric and magnetic fields at the frequencies of interest (using finite element methods) are used to judge the nature of the electromagnetic response of the medium.

Figure 1 shows a schematic representation of the unit cell of the symmetric SRR, with two capacitive gaps. The electromagnetic response of this structure as a function of the gap width d is presented in this section. The unit cell considered in our calculations is a square with side $a = 300$ nm in each case. The width of each of these SRR structures is 24 nm across and the length of the sides $b = 180$ nm. The evolution of the SRR response with changing capacitance has been presented. The response of these systems has been calculated using the PHOTON codes [13,14] based on the transfer matrix method. These calculations are essentially two-dimensional with the magnetic field being aligned along the axis of invariance of the system (the y-axis), normal to the plane of the SRRs. Experimentally obtained values were used for the bulk permittivity of silver [15], the constituent metal of the SRRs. The cross-sections of the SRR has been chosen to be square in order to avoid the staircasing effects that would have resulted from simulating circular SRRs on a square grid. Typically, seventy-five grid points along each direction were used to accurately model the response of the system. The homogenizable metamaterials were assigned an effective permeability using the procedure described by Koschny *et al* [16]. Eight different situations have been studied, beginning with hollow square cylindrical structures to plate pairs oriented perpendicular to the electric field of the incident radiation.

(i) The first case considered is the response of an array of hollow square cylinders. This system may have a net diamagnetic response with μ_{eff} taking up values

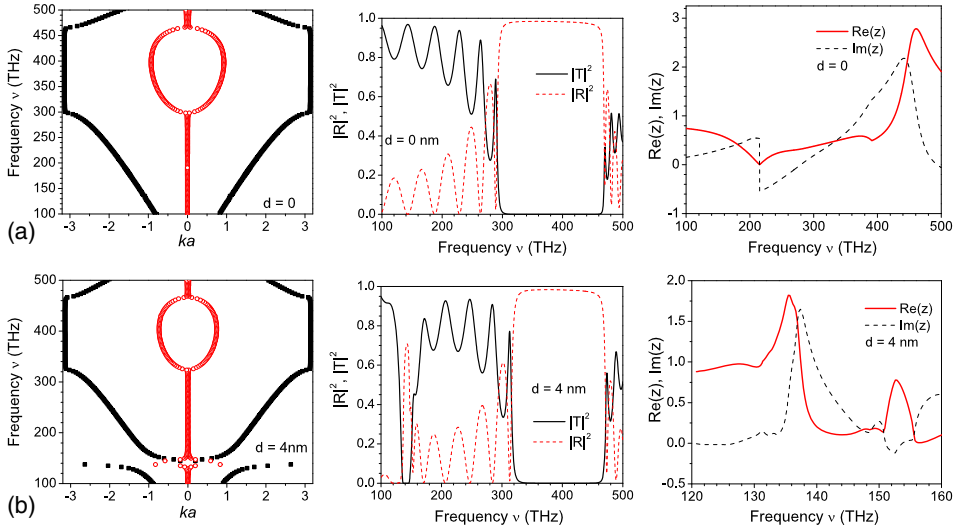

Figure 2. (Left) Band structures for the SRR shown in figure 1 as the gap width increases from 0 to 4 nm. A negative permeability band gap due to a magnetic resonance appears when $d = 4$ nm. (Middle) The reflectivity and the transmittivity for a slab consisting of two layers of SRRs, whose capacitive gaps correspond to $d = 0$ and 4 nm, respectively. (Right) The calculated impedance Z for the gap widths of 0 and 4 nm, respectively.

which are positive but <1. This is simply the analogue of the array of cylinders which shows a net diamagnetic response, but with a square rather than a circular cross-section. Although the array exhibits a single large band gap extending from 290 THz to 483 THz, this band gap cannot be attributed to a negative effective permeability [4]. A plot of the spectrum of the reflectivity and the transmittivity of the system (for two layers of unit cells) (figure 2, top panel) shows that the transmittivity drops to nearly zero from about 80% at approximately 299 THz and remains at this level upto frequencies of 483 THz before rising again to levels of 70%. As expected in the case of a layered system, Fabry–Pérot resonances occurring as a result of multiple scattering from the edges of the layers, are seen both below and above this band gap. The effective impedance of this structure is low near the lower band edge, suggesting that the effective permittivity of the medium is high, a feature that is associated with a dielectric resonance, for this system. However, since the wavelength of the radiation is nearly $\lambda/3$, the effective medium approach cannot be applied straightforwardly and we do not attribute an effective permittivity. However, due to the subwavelength size, Bragg scattering is also not expected to dominate. The focussing of TM-polarized light by an array of such hollow cylinders (discussed in ref. [12]) suggests a negative dielectric permittivity for this system. The negative permittivity probably arises due to the coupling of the electric dipoles formed in adjacent unit cells by the electric field, a behaviour akin to the cut-wire system [17].

(ii) Next, the response of a slab consisting of split ring with two splits opposite to each other (where each split is 4 nm wide), is presented (figure 2, bottom panel). The band structure of this medium shows the occurrence of two band gaps, one around 121 THz and the other at ∼289 THz. The lower (narrower) gap in this case is easily identified as the negative permeability band gap of the SRR (due to the classical LC resonance in the ring) while the one at higher frequencies is due to the same mechanism the band gap encountered in case (i). The transmittivity of the slab drops nearly to zero from about 85% near 132 THz and remains nearly zero till 152 THz when it rises, exhibits a series of Fabry–Pérot resonances and then again shows a region of very low transmittivity from 289 THz to 483 THz, just like the one observed in the case of the hollow structure. The first stop band is a region where the impedance of the system is high, compared to the second stop band where the effective impedance is low. This high impedance is typical of the SRR-based metamaterials, which have a high magnetic permeability at resonance. At the frequency where the first band gap is formed, the medium is homogenizable ($a \sim \lambda/8$) and effective parameters can be extracted. The retrieved permeability shows a negative μ band at the location of the first gap.

(iii) In the third case, the widths of the capacitive gaps of the SRRs are increased to $d = 12$ nm. Once again, two band gaps are seen (shown in figure 3, top panel). The first band gap now occurs at a higher frequency (due to the reduced capacitance of the SRR) while the second band gap too shifts upwards and narrows

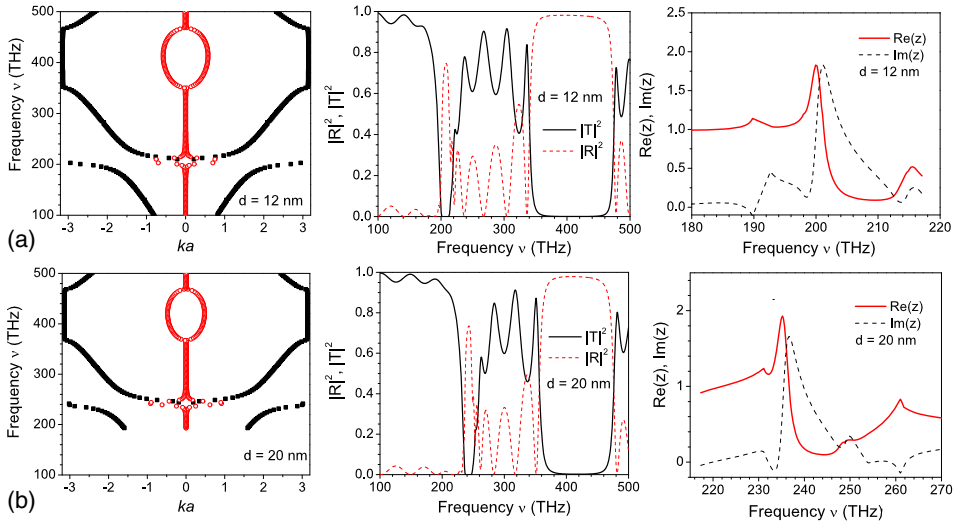

Figure 3. (Left) Band structures for the SRR shown in figure 1 as the gap width is increased to 12 nm and 20 nm. The negative permeability band gap moves towards higher frequencies. (Middle) The reflectivity and the transmittivity for a slab consisting of two layers of SRRs, whose capacitive gaps correspond to $d = 12$ and 20 nm, respectively. (Right) The calculated impedance Z for the gap widths of 12 and 20 nm, respectively.

down as well. The upper edge of the second band gap, however, remains at 483 THz. The lower gap is the narrower of the two. The reflectivity–transmittivity profile of this system is similar to the previous one with two stop bands where the first narrow band is the usual SRR negative μ-band while the second is the same stop band seen in Cases (i) and (ii). The lower edge of the second stop band also shows a slight upward shift. The effective permeability in the first gap (where $a \sim \lambda/7$) is negative, confirming that it arises due to the LC resonance of the SRR.

(iv) In this case, the capacitive gap width of the SRR is increased to 20 nm. The response of an array of such SRR is shown in figure 3, bottom panel. The calculated band structure for an array of such SRRs shows two bands as before, with the first one progressively having moved upwards in frequency and the band width narrowing in extent. The second one also shifts upward in frequency but its upper edge remains unaltered at 483 THz. The reflectivity–transmittivity spectrum for a double layered slab of these SRRs is qualitatively similar to those obtained in Cases (ii) and (iii). The negative permeability band is at a higher frequency as the capacitance is lowered again while the second stop band is not much altered. The unit cell $a \sim \lambda/4$ at the resonance. At these length scales, the interaction of the electric field of the incident radiation with the SRR itself is expected to strongly affect the retrieved parameters, and this is the frequency regime where the effective medium theories weaken considerably.

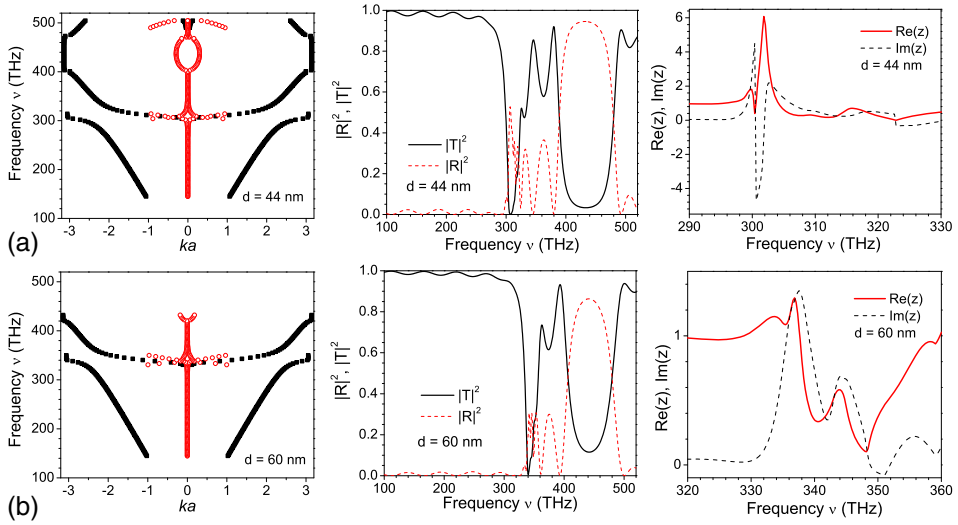

Figure 4. (Left) Band structures for the SRR shown in figure 1 as the gap width increases to 44 nm and 60 nm. The negative permeability band narrows and moves upwards with increasing gap width d. (Middle) The reflectivity and the transmittivity for a slab consisting of two layers of SRRs, whose capacitive gaps correspond to $d = 44$ and 60 nm, respectively. (Right) The calculated impedance Z for the gap widths of 44 and 60 nm, respectively.

(v) In this case, we present SRRs whose capacitive gaps have a width of 44 nm each. The net capacitance of the structure is reduced substantially and the first band gap is pushed high up in frequency such that a is only slightly greater than $\lambda/3$ (see figure 4, top panel). The lower stop band narrows down and almost disappears due to the weakening of the SRR resonance. The large capacitive gap prevents strong capacitive coupling between the two parts of the SRR. Homogenization becomes truly problematic here. The second gap occurring at higher frequencies is still prominent although it, too, narrows down. The plots of the reflectivity and the transmittivity of a double layer of unit cells still show the considerably weakened SRR stop band. In the region of the second stop band, the transmittivity drops to around 30%, compared to the near-zero values obtained in the earlier cases. A comparison of the reflectivity and the transmittivity spectra shows that the behaviour of the system has changed considerably from that seen in (ii), (iii) and (iv).

(vi) In this case, the widths of the capacitive gaps, $d = 60$ nm. From the band structure, it is evident that the lower band due to the magnetic resonance and the upper bands nearly intersect (figure 4, bottom panel). The second gap also narrows further, leading one to suspect that the physical phenomena responsible for the original gap formation, such as the coupling between adjacent cells, are ceasing to be dominant. The reflectivity and the transmittivity for two layers of unit cells of the SRR show a clearer manifestation of this phenomenon. The first stop band is weaker while the second one changes considerably in character. Instead of

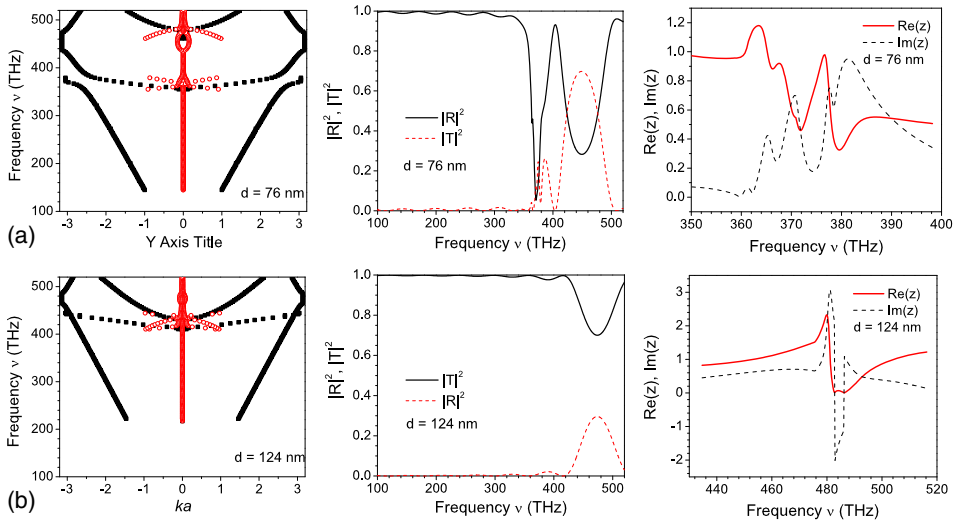

Figure 5. Band structures for the SRR shown in figure 1 as the gap width increases to 76 nm and 124 nm. The negative permeability band gradually disappears with increasing gap width. (Middle) The reflectivity and the transmittivity for a slab consisting of two layers of SRRs, whose capacitive gaps correspond to $d = 76$ and 124 nm, respectively. (Right) The calculated impedance Z for the gap widths of 76 and 124 nm, respectively.

another stop band, we find that both the reflectivity and the transmittivity drop to about 50%. Evidently, the phenomena which influenced the response of the system earlier are now being replaced by another set. The two band frequencies are now close to each other and we are gradually approaching the limit where Bragg scattering begins to dominate (i.e., when $a \sim \lambda/2$).

(vii) In the next stage, the gaps are further increased to 76 nm. Due to the lowered capacitance of the structure, the lower band is pushed further upwards, resulting in the disappearance of the first band gap. The higher band gap narrows as well. The reflectivity–transmittivity profile changes completely, with only one narrow stop band being seen at the point where both the band frequencies overlap (figure 5, top panel).

(viii) Finally, the extreme case when the legs constituting the capacitances are completely removed, corresponds to the case of plate pairs and is discussed in the next section.

3. Comparative study of plate-pair structures

We now compare the behaviour of two types of plate-pair structures. In the first case [12], the pairs are considered to be aligned perpendicular to the electric field of the incident radiation. In this case, one obtains a nearly gapless dispersion with a negative phase velocity over a large band. Negative phase velocity bands are obtained as the fact that the real and imaginary parts of the wave-vector have opposite signs indicates. At these frequencies, the free space wavelength of the light is about thrice the size of the unit cell and only one transmitted and reflected beam is obtained from a slab of such SRRs as all other higher-order diffracted beams are evanescent. Interestingly, the band structure for the plate pairs in figure 6 rotated by $\pi/2$ (shown in figure 5), is again completely different.

In the second case, the SRR system is reduced to a pair of plates parallel to each other, 124 nm apart and aligned parallel to the electric field of the incident radiation. The bands

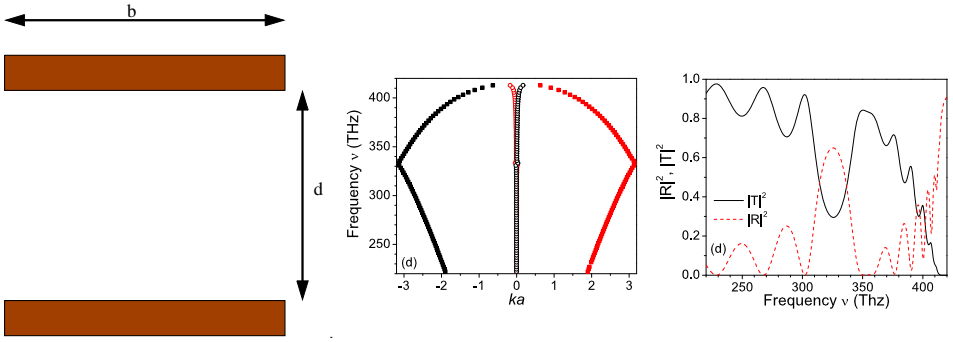

Figure 6. (Left) A paired plate structure obtained from the SRR shown in figure 1 with a gap width of 124 nm oriented along the electric field. (Middle) The calculated band structure for the plate pair structure in this orientation. (Right) The reflectivity and the transmittivity corresponding to this band structure.

Table 1. The changing nature of the response of the SRR whose structure has been shown in figure 1 as the gap width d varies.

SRR	Figure No.	Gap width (nm)	Resonance (1) (THz)	Resonance (2) (THz)	Nature of resonance
i	Figure 2	0	None	300	(1) None (2) Electric
ii	Figure 2	4	138	326	(1) Magnetic (2) Scattering
iii	Figure 3	12	204	350	(1) Magnetic (2) Scattering
iv	Figure 3	20	238	370	(1) Magnetic (2) Scattering
v	Figure 4	44	304	400	(1) Magnetic (2) Scattering
vi	Figure 4	60	340	420	(1) Magnetic (2) Scattering
vii	Figure 5	76	370	447	(1) None (2) Electric
viii	Figure 5	124	None	466	(2) None (2) Electric

for this structure actually intersect at ∼459 THz. The plots of the reflectivity and the transmittivity are completely featureless, except for a drop in transmission and an accompanying increase in reflection at ∼483 THz (figure 5, bottom panel). This frequency corresponds to $a \sim \lambda/2$. Here, the only phenomenon expected is Bragg scattering. All other resonant effects, whether it is the LC resonance seen in SRR systems due to their geometric structure, or those arising from plasmonic effects, are completely wiped out. This band structure is thus completely different from the one exhibited by the plate pairs oriented orthogonal to the electric field of the incident radiation. The plate pairs shown here are highly transmittive in the frequency range around ∼435 THz. This is in sharp contrast with the behaviour of the structure shown in figure 6 (left). Moreover, the plates are aligned parallel to the electric field of the incident radiation which can allow them to behave in a plasma-like fashion like the cut wire media described earlier.

4. Conclusions

In conclusion, we have numerically studied the nature of the localized resonances of split-ring resonator metamaterials as a function of the size of the unit cell to wavelength (a/λ) ratio. At low resonance frequencies, the homogenization conditions are satisfied and the classical effective medium description of this metamaterial is valid. At high frequencies, when the size of the unit cell of the SRR is a significant portion of the wavelength, such a description as a homogeneous medium is not valid. The nature and symmetry of the localized resonances of the single units still give important clues to the properties of the metamaterial. At high frequencies, the Bragg scattering in the medium becomes the

dominant mechanism for a band gap and the properties of the structured medium is dominated by it. The principal results regarding the nature of the resonance of the SRR with increasing frequency are summarized in table 1.

Acknowledgements

The authors acknowledge funding from the US Air force AFOSR/AOARD by Grant No. AOARD-09-4042

References

[1] V G Veselago, *Usp. Fiz. Nauk* **92**, 517 (1967); *Sov. Phys. Usp.* **10**, 509 (1968)
[2] S A Ramakrishna and T M Grzegorczyk, *Physics and applications of negative refractive index materials* (CRC Press, Boca Raton, 2009)
[3] S A Ramakrishna and O J F Martin, *Opt. Lett.* **30**, 2626 (2005)
[4] J B Pendry, A J Holden, D J Robbins and W J Stewart, *IEEE Trans. Microwave Theory Tech.* **47**, 2075 (1999)
[5] D R Smith, W J Padilla, D C Vier, S C Nemat-Nasser and S Schultz, *Phys. Rev. Lett.* **84**, 4184 (2000)
[6] I Sersic, M Frimmer, E Verhagen and A F Koenderink, *Phys. Rev. Lett.* **103**, 213902 (2009)
C M Soukoulis, S Linden and M Wegener, *Science* **315**, 47 (2007)
V M Shalaev, *Nat. Photon.* **1**, 41 (2007)
[7] S Zhang, W Fan, N C Panoiu, K J Malloy, R M Osgood and S R J Brueck, *Phys. Rev. Lett.* **95**, 137404 (2005)
[8] D Schurig, J J Mock, B J Justice, S A Cummer, J B Pendry, A F Starr and D R Smith, *Science* **314**, 977 (2006)
[9] J B Pendry, D Schurig and D R Smith, *Science* **312**, 1780 (2006)
[10] S O'Brien and J B Pendry, *J. Phys.: Condens. Matter* **14**, 6383 (2002)
[11] S O'Brien, D McPeake, S A Ramakrishna and J B Pendry, *Phys. Rev.* **B69**, 241101(R) (2004)
[12] Sangeeta Chakrabarti and S A Ramakrishna, *J. Nonlinear Opt. Phys. Mater.* **17**, 143 (2008)
[13] J B Pendry and A MacKinnon, *Phys. Rev. Lett.* **69**, 2772 (1992)
[14] J B Pendry, *J. Mod. Opt.* **41**, 209 (1994)
[15] P B Johnson and R W Christy, *Phys. Rev.* **B6**, 4370 (1972)
[16] Th Koschny, P Markoš, D R Smith and C M Soukolis, *Phys. Rev.* **B65**, 195104 (2002)
[17] Th Koschny, P Markoš, D R Smith and C M Soukoulis, *Phys. Rev.* **E68**, 065602 (2003)